
Proceedings Paper:
Calautit, J.K. and Hughes, B.R. (2015) Application of a Passive Cooling Wind Catcher within the Built Environment: Numerical and Experimental Analysis. In: Proceedings of the SusTEM2015 conference. SusTEM2015, Newcastle, UK. Newcastle University.

Application of a Passive Cooling Wind Catcher within the Built Environment: Numerical and Experimental Analysis

John Kaiser Calautit [a*], Ben Richard Hughes [a]

[a] Department of Mechanical Engineering, University of Sheffield, Sheffield, S10 2TN, United Kingdom
* Corresponding author. Email:j.calautit@sheffield.ac.uk; Tel. +44(0) 7544158981

Abstract
Commercial wind catchers are passive ventilation devices adapted from vernacular architecture of Middle Eastern cultures which date back hundreds of years. The wind catcher sustain natural ventilation and cooling in buildings through wind driven airflow as well as temperature difference. However, its cooling performance is limited in hot climates, especially during the summer period. In this study, a standard roof-mounted wind catcher was integrated with heat pipes to reduce the temperature of the supply airflow. A commercial CFD code was used to simulate the effect of the heat pipes on the ventilation and thermal performance of the system. A 1:10 scale model was created using a 3D printer and tested inside a low-speed wind tunnel. Qualitative and quantitative wind tunnel analysis of the airflow through the wind catcher were compared with the CFD results. Field testing of the wind catcher was also conducted in the Middle East to evaluate its performance under real conditions. A cooling potential of up to 12K was identified in this study. The technology presented here is subject to an international patent application (PCT/GB2014/052263).

Keywords: CFD modelling; field testing; hot climates; natural ventilation; sustainable buildings

1 Introduction
There is a large reliance on electricity to run mechanical systems to provide ventilation and thermal comfort in buildings situated in hot regions. Commercial and residential buildings are responsible for 40 % of the world energy usage as well as 40-50 % of the global carbon emissions [1]. Heating Ventilation and Air Conditioning (HVAC) systems consume more than 60 % of the total energy use in buildings [2]. This represents a significant opportunity for reducing the energy consumption and greenhouse gas emissions. Natural ventilation devices such as wind catchers are increasingly being employed in building design for increasing fresh air rates and reducing energy consumption [3, 4]. An example of this ventilation device is the Malqaf (Figure 1a), a uni-directional wind catcher which is a shaft projecting on the roof. It has a large opening facing the predominant wind that captures the air from high elevation and directs it downward into the room [5]. Figure 1b demonstrates the operation of a Malqaf wind catcher as part of a complete ventilation system, which includes an air escape roof that extracts the air out of the building. The system primarily depends on the air movement caused by the pressure differential, although convection produces the stack effect aswell.

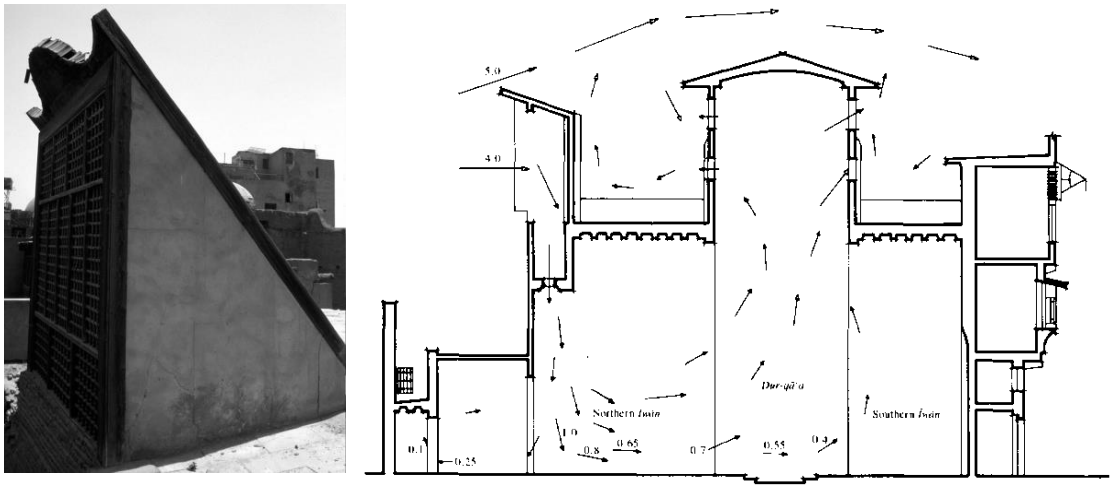

Figure 1: *A traditional Malqaf wind catcher (left) airflow through a building with Malqaf (right) [5].*

1.1 Literature review

A number of works [6-15] have investigated the performance of wind catchers using numerical and experimental analysis. Attia and Herde [8] assessed the ventilation performance of a uni-directional wind catcher used in residential buildings. Wind tunnel and flow visualisation testing were carried out to evaluate the airflow rate and distribution in a room integrated with the wind catcher. The result indicated that a single uni-directional wind catcher was capable of supplying up to 4 ACH (air change per hour). Montazeri and Azizian [9] evaluated the performance of a similar wind catcher using wind tunnel and smoke testing. A scale model of the ventilation device was mounted to a room which was installed beneath the base of the ventilation device. Results showed that the one-sided wind catcher had the potential to be provide ventilation in urban settings.

Traditional wind catchers were integrated with evaporative cooling devices to increase its thermal performance [11-15]. Bahadori *et al.* [10] evaluated the cooling performance of two designs of wind catchers using experimental testing. The two designs were one with wetted columns, equipped with cloth curtains suspended in the channel and one with wetted surfaces was equipped with cooling pads at the entrance. The results indicated that the device with wetted column was more effective during high wind conditions, while the device with wetted surfaces was more effective during low wind conditions. Safari and Hosseinnia [11] used CFD modeling to investigate the thermal performance of new designs of wind catchers with wetted columns. The numerical results showed that the wetted columns with the height of 10 meters were able to reduce the air temperature by 12 K.

Bouchahm *et al.* [12] evaluated the ventilation and thermal performance of a wind catcher incorporated to a building using experimental analysis. Clay conduits were mounted inside the shaft of the device to improve the heat transfer and a water pool was situated at the bottom of the device. Kalantar [13] evaluated the performance of a wind catcher with evaporative cooling spray in the hot region of Yazd using CFD. It was found that the wind catcher was able to reduce the air temperatures by 10 to 15°C at its optimum performance. Using the same CFD method, Calautit *et al.* [14] compared the thermal performance of an evaporative cooling and heat pipe assisted cooling for traditional wind catchers. The heat pipe system works on a similar principle of providing cooling but unlike evaporative cooling, which directly evaporates water to the airstream, a heat pipes is an indirect cooling devices Therefore, there is less increase in humidity compared to evaporative cooling techniques, making it viable for regions with moderate humid conditions. There is also less risk of contamination of the airstream (for example, waterborne bacterias). Furthermore, the study concluded that height was not a factor for the heat pipe integrated wind catcher, making it viable for commercial devices.

1.2 Objectives

In our previous works [14, 15], we evaluated the integration of heat pipes into traditional and modern wind catchers. The results showed that the system was capable of reducing the temperature and supplying the recommended fresh air rates. Although, the previous analysis were completely CFD-based and assessment by experimental methods was of further interest. This study will use CFD, wind tunnel and field-test analysis to address the gap in the literature.

Figure 2 shows the operation of the proposed wind catcher with heat pipes. The hot outdoor air enters the wind catcher through the louvers which are used to deflect the impact of weather, noise, direct sunshine and other small objects from entering the wind catcher. The airflow is driven downwards and passed through a series of heat pipes which absorbs the heat from the airflow (evaporator) and transfers it to a parallel cool sink (condenser). The heat pipe is a simple device of very high thermal conductivity with no moving parts that can transport large quantities of heat efficiently over large distances fundamentally at an invariable temperature without requiring any external electricity input. It is essentially a conserved slender tube containing a wick structure lined on the inner surface and a small amount of fluid such as water at the saturated state. Adjustable dampers are mounted at the bottom of the unit to control the delivery rate of the outdoor air, as fluctuations in external wind speed greatly influence the air movement rate within the occupied space. The cooled air is supplied to the room beneath the channel via the ceiling diffusers.

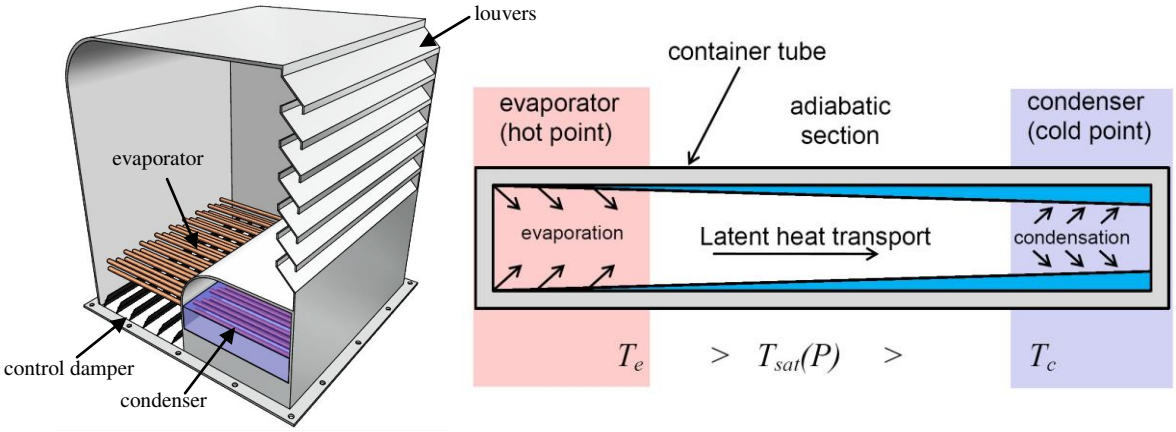

Figure 2: *Wind catcher with heat pipes (left) heat pipe operation (right)[16].*

2 Methodology

2.1 Numerical modelling

The basic assumptions for the numerical simulation include a three-dimensional, fully turbulent, and incompressible flow. The internal and external flow was modeled by using the standard k–epsilon turbulence model, which is a well-established method in research on natural ventilation [4, 17-20]. The CFD code was used with the Finite Volume Method (FVM) approach and the Semi-Implicit Method for Pressure-Linked Equations (SIMPLE) velocity-pressure coupling algorithm with the second order upwind discretisation. The general governing equations include the continuity (eqn.1), momentum (eqn.2) and energy (eqn.3) balance for each individual phase. The standard k-e transport model was used to define the turbulence kinetic energy and flow dissipation rate within the model. The transport equations are formulated in eqn.4 and eqn.5.

$$\frac{\partial}{\partial t}(\alpha_q \rho_q) + \nabla \cdot (\alpha_q \rho_q \vec{v}_q) = \sum_{p=1}^{n} (\dot{m}_{\mathrm{pq}} - \dot{m}_{\mathrm{qp}}) + S_q \tag{1}$$

$$\frac{\partial}{\partial t}(\alpha_q \rho_q \vec{v}_q) + \nabla \cdot (\alpha_q \rho_q \vec{v}_q \vec{v}_q) = -\alpha_q \nabla p + \nabla \cdot \bar{\bar{\tau}}_q + \alpha_q \rho_q \vec{g} + \sum_{p=1}^{n} (\vec{R}_{pq} + \dot{m}_{pq} \vec{v}_{pq} - \dot{m}_{qp} \vec{v}_{qp}) + (\vec{F}_q + \vec{F}_{\mathrm{lift},q} + \vec{F}_{\mathrm{vm},q}) \tag{2}$$

$$\frac{\partial}{\partial t}(\alpha_q \rho_q h_q) + \nabla \cdot (\alpha_q \rho_q \vec{u}_q h_q) = \alpha_q \frac{\partial p_q}{\partial t} + \bar{\bar{\tau}}_q : \nabla \vec{u}_q - \nabla \cdot \vec{q}_q + S_q + \sum_{p=1}^{n} (Q_{pq} + \dot{m}_{pq} h_{pq} - \dot{m}_{qp} h_{qp}) \tag{3}$$

where; $\vec{v}_q$ represents the velocity of phase q and $\dot{m}_{pq}$ and $\dot{m}_{qp}$ characterizes the mass transfer from the pth to qth phase and vice-versa. $\bar{\bar{\tau}}_q$ represents the qth phase stress-strain tensor. h_q represents the specific enthalpy of the qth phase and $\vec{q}_q$ represents the heat flux. Q_{pq} represents the intensity of heat exchange between the pth and qth phases and h_{pq} is the interface enthalpy. S_q represents the source term.

$$\frac{\partial}{\partial t}(\rho k) + \frac{\partial}{\partial x_i}(\rho k u_i) = \frac{\partial}{\partial x_j}\left[\left(\mu + \frac{\mu_t}{\sigma_k}\right)\frac{\partial k}{\partial x_j}\right] + G_k + G_b - \rho\epsilon - Y_M + S_k \tag{4}$$

$$\frac{\partial}{\partial t}(\rho \epsilon) + \frac{\partial}{\partial x_i}(\rho \epsilon u_i) = \frac{\partial}{\partial x_j}\left[\left(\mu + \frac{\mu_t}{\sigma_e}\right)\frac{\partial e}{\partial x_j}\right] + C_{1\epsilon}\frac{\epsilon}{k}(G_k + C_{3\epsilon}G_b) - C_{2\epsilon}\rho\frac{e^2}{k} + S_\epsilon \tag{5}$$

where; G_k represents the generation of turbulence kinetic energy due to the mean velocity gradients, G_b represents the generation of turbulence kinetic energy due to buoyancy. Y_M represents the contribution of fluctuating dilatation in compressible turbulence to the overall dissipation rate. $C_{1\epsilon}$, $C_{2\epsilon}$ and $C_{3\epsilon}$ are constants, σ_k and σ_e are the turbulent Prandtl numbers for k and Ɛ. S_k and S_ϵ are the source terms.

2.2.1 Computational domain and mesh

The wind catcher geometry (Figure 3) was created using a commerical CAD software and then imported into ANSYS Geometry (pre-processor) to create a computational model. The solid parts of the wind catcher and test room geometry were created using the CAD software. However, replicating the physical geometry of the wind catcher does not represent a computational domain. To create a computational domain, the fluid volume was extracted from the solid model as shown in Figure 4. The fluid domain was separated into three parts: the macro-climate (outdoor), wind catcher and micro-climate (indoor). The macro-climate was created to simulate the outdoor airflow. The macro-climate consisted of an inlet on one side of the domain, and an outlet on the opposing boundary wall. The macro-climate dimensions was 5 m x 5 m x 10 m. According to the dimensions of the wind catcher (1 m x 1 m x 1 m), the model produced a blockage of 4.8 %. The wind catcher was incorporated to a micro-climate with the dimensions of 3 m x 5 m and 5 m, representing a small room [17, 18]. The wind catcher was modelled with seven louvres angled at 45°. The wind catcher was assumed to be supplying at 100 % (fully open), therefore the volume control dampers was not added to the model. The cylindrical heat pipes, each with an outer diameter of 0.02 m, were integrated in to the lower part of the channel as shown in Figure 3. The horizontal distance between each pipe was 0.05 m.

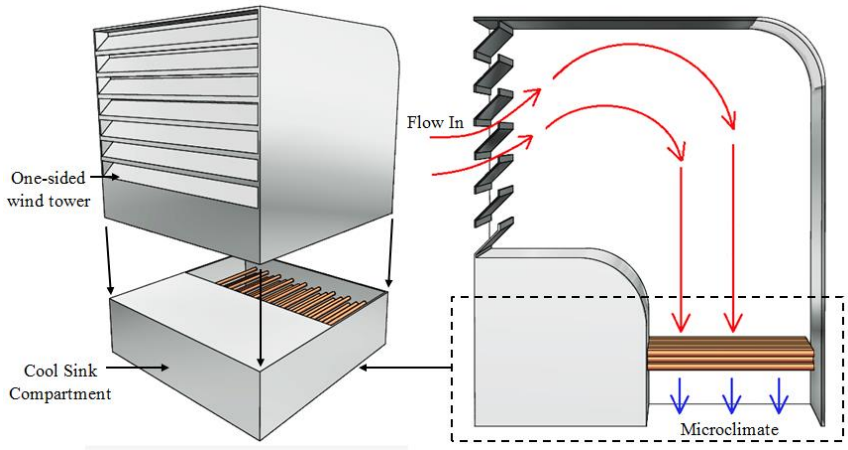

Figure 3: *CAD model of the wind catcher with cylindrical heat pipes.*

Due to the complexity of the model, a non-uniform mesh was applied to volumes of the computational domain [19]. The generated computational mesh of the wind catcher and room model are shown in Figure 4. The grid was modified and refined according to the critical areas of interests in the simulation such as the heat pipes. The size of the mesh element was extended smoothly to resolve the areas with high gradient mesh and to improve the accuracy of the results. The inflation parameters were set according to the complexity of the geometry face elements, in order to generate a finely resolved mesh normal to the wall and coarse parallel to it [19].

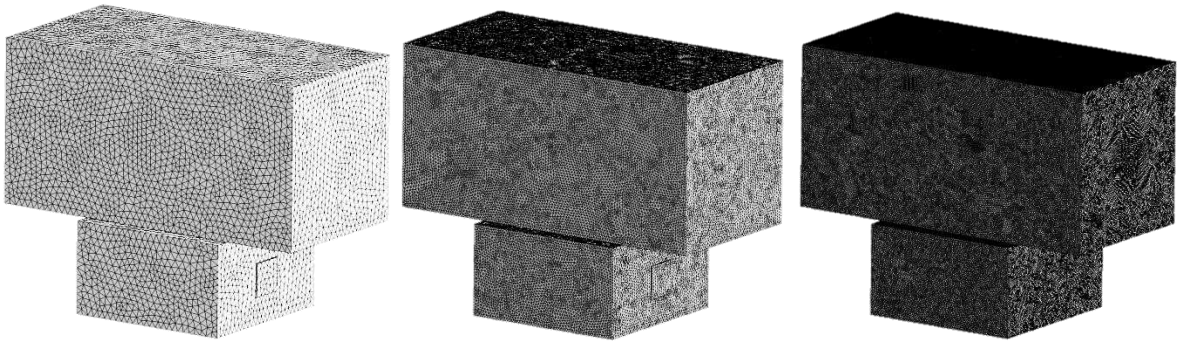

Figure 4: *Mesh refinements: 1 million, 2.1 million and 4.9 million cells*

Mesh adaptation was used to verify the computational mesh of the wind catcher and room model. The process increased the number of elements between 1 and 7.2 million. Each stage continued until an acceptable compromise was reached between: number of elements; computational time to solve; and

the posterior error indication. At 4.9 million elements the error indication between refinements was at its lowest; coupled with the computational time, made it an acceptable compromise. Figure 4 shows the stages of refinement from 1 million to 4.9 million elements.

2.2.2 Boundary conditions

The boundary conditions for the CFD model are summarised in Table 1.

Table 1: Summary of the CFD model boundary conditions.

Boundary condition	***Set value***
Discretisation Scheme	*Second order upwind*
Algorithm	*SIMPLE*
Time	*Steady State*
Viscous model	*k-epsilon two equation*
Velocity inlet	*1-5 m/s*
Pressure outlet	*Atmospheric*
Gravity	*-9.81*
External temperature	*318 K*
Heat pipe temperature	*293 K*

2.2 Experimental wind tunnel testing

A 1:10 scale model of the wind catcher was used in the experimental study. The investigation was conducted in a closed-loop wind tunnel detailed in [21]. The wind tunnel had a test section with the dimensions of 0.5, 0.5, and 1 m (Figure 5). According to the dimensions of the 1:10 model and the wind tunnel cross-section, the wind catcher scale model produced a wind tunnel blockage of 4.8%, and no corrections were made to the measurements obtained with these configurations [22, 23]. The creation of an accurate scaled wind tunnel prototype was essential for the experimental study. Therefore, the model of wind tunnel was constructed using 3D printing. Figure 5 shows the 3D printed 1:10 wind catcher scale model design. The model of the wind catcher was connected to a 0.5 x 0.5 x 0.3 m room, which was mounted underneath the test section. A single 0.1 x 0.1 m outlet window was located at the leeward side of the room. The test room was made of acrylic perspex sheet to facilitate the flow visualisation of the airflow. In order to test the impact of different wind directions, the top plate of the test room was constructed with an ability to be rotated in the test section.

The airflow into the room was measured using a hot-wire anemometer, which was positioned below the channels of the wind catcher. The cross-sectional area of the wind catcher was divided into several portions and the supply rate through the channel was calculated. The hot-wire sensor gave airflow velocity measurements with uncertainty of ±1.0 % rdg. at speeds lower than 8 m/s and uncertainty of ±0.5 % rdg. at higher speeds (8 – 20 m/s).

Figure 5: *Low-speed wind tunnel (left) 3D printed model (right) [24, 25].*

2.3 Experimental field testing

Experimental field testing of the wind catcher with heat pipes was carried out to evaluate its performance under real operating conditions. A prototype of the wind catcher was produced and mounted on top of a 3 m x 3 m x 3 m test room on an open field site in Ras Al Khaimah, UAE. Figure 6 shows the site location and the test setup. Ras Al Khaimah is located at latitude 25.78˚N and longitude 55.95 ˚E. Its climate can be characterised as a hot-desert climate. High temperatures can be expected from June to September, with a maximum temperature ranging between 312 K and 315 K and a minimum temperature ranging between 297 K and 303 K. The predominant wind angle is between North and North-West direction. Therefore, the opening of the wind catcher was positioned to face the predominant wind. The average wind velocity is between 3 m/s and 4 m/s.

The experimental tests were carried out during the month of September, between 11:00 AM and 4:00 PM (highest outdoor air temperatures). The test room was constructed from insulated studwork (weather-proofed). An opening located on the leeward side of the room was used as an outlet. The prototype was constructed using aluminum plate with a thickness of 3 mm. The overall dimension of the wind catcher was 1 m x 1 m x 1.2 m. A total of 50 cylindrical heat pipes (each with an outer diameter of 0.02 m and total length of 0.95 m) and a parallel cold sink (fed by water at approximately 288 K - 293 K) were incorporated into the wind catcher to provide the cooling.

Figure 6: *Test site in Ras Al-Khaimah (top) wind catcher mounted on the roof (bottom left) measurement setup (bottom right).*

3 Results and discussion

3.1 Numerical simulation results

Figure 7 illustrates a cross-sectional plot of the velocity contours in the room and wind catcher with heat pipes. The right hand side of the plot shows the scale of airflow velocity (m/s). The contour plot in the fluid domain is colour coded and related to the CFD colour map, ranging from 0 to 3.7 m/s. As observed, the airflow passed around the wind catcher, parts of it entered the wind catcher and parts of it exited through the pressure outlet on the right side of the domain. After entering the wind catcher, the airflow was accelerated as it hit the rear wall of the channel and re-directed downward towards the room. Separation zone was observed near the lower edge of the opening, which caused a sharp variation in velocity in this region and reduced the maximum efficiency of the wind catcher. High draft speeds were observed at the centre of the room reaching up to 0.83 m/s. The air stream was circulated inside the structure and exited the opening located on the leeward side of the room. The average air velocity inside the room model was 0.28 m/s.

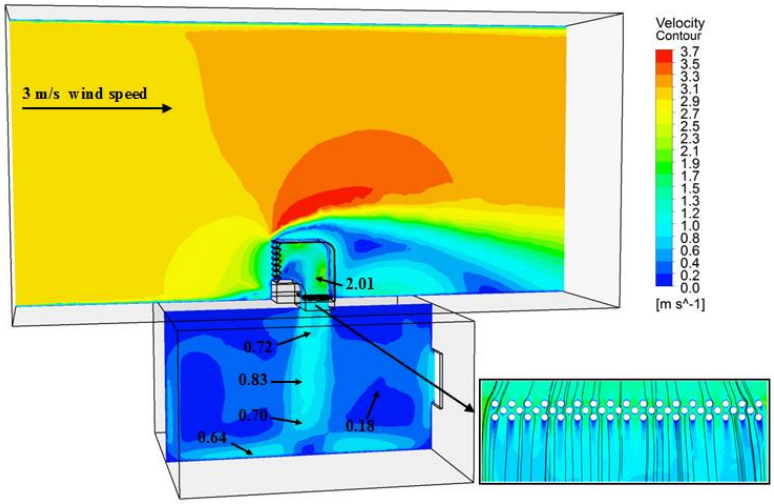

Figure 7: *Cross-sectional plot of the velocity contours.*

Figure 8 displays a cross-sectional plot of the temperature distribution inside the room with a wind catcher. The right hand side of the contour plot shows the scale of static temperature (K). The contour plot in the fluid domain is colour coded and related to the CFD colour map, ranging from 293 K to 318 K. The average temperature inside the room was 310.4 K when the temperature of the outdoor wind was set at 318 K. The temperature was reduced further at the immediate downstream of the heat pipes with a supply temperature value of 309 K. Figure 9 shows the effect of the variation of wind speed on the thermal performance of the wind catcher system.

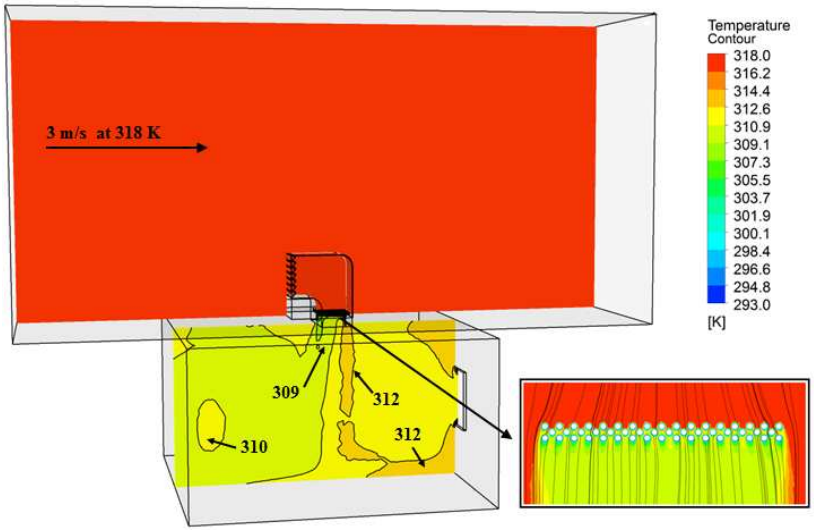

Figure 8: *Cross-sectional plot of the static temperature contours.*

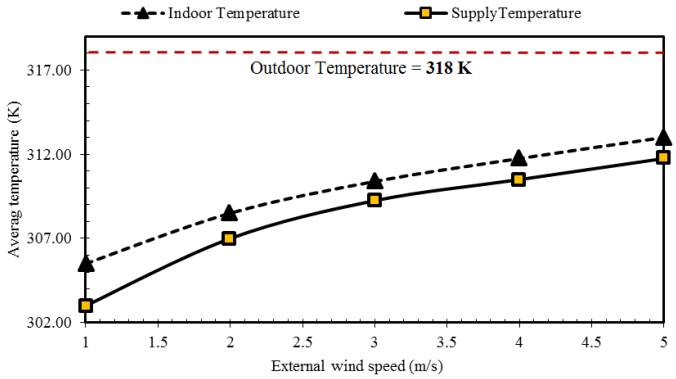

Figure 9: *Effect of wind speed on supply and indoor temperature.*

3.2 Wind tunnel test results

Figure 10 shows the comparison between the predicted and experimental results for the airflow velocity measurements below the wind catcher channel. An uneven airflow distribution was observed below the supply channel. The airflow speed on the right corner of the channel (Points 1, 4 and 7) was 30 – 60 % higher than the left corner (Points 3, 6 and 9). This was due to the flow separation created by the sudden change in direction (90˚ bend). Good agreement was observed between the CFD results and measurement, with the error below 10 % for all the points except for point 6. The average error across the points was 7.2 %. Figure 11 compares the smoke testing results with the CFD flow visualisation.

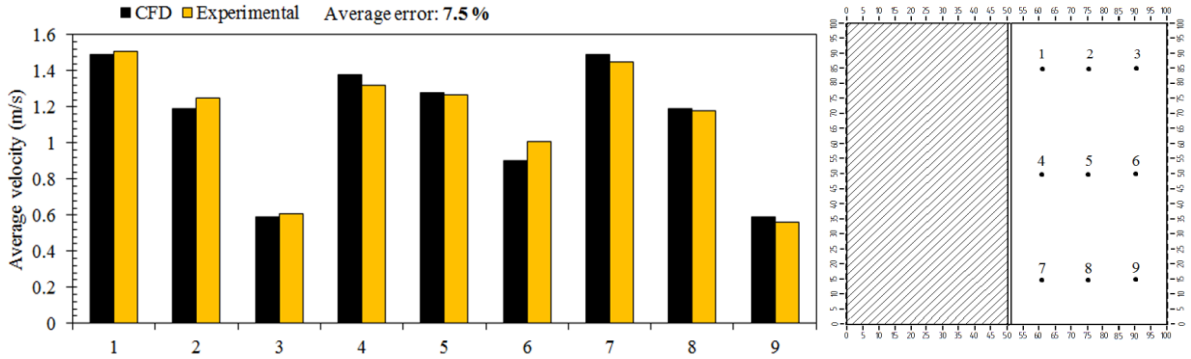

Figure 10: *(a) Comparison between the prediction of the CFD and the measurement of the airflow speed at different points (b) location of measurement points inside the wind catcher diffuser*

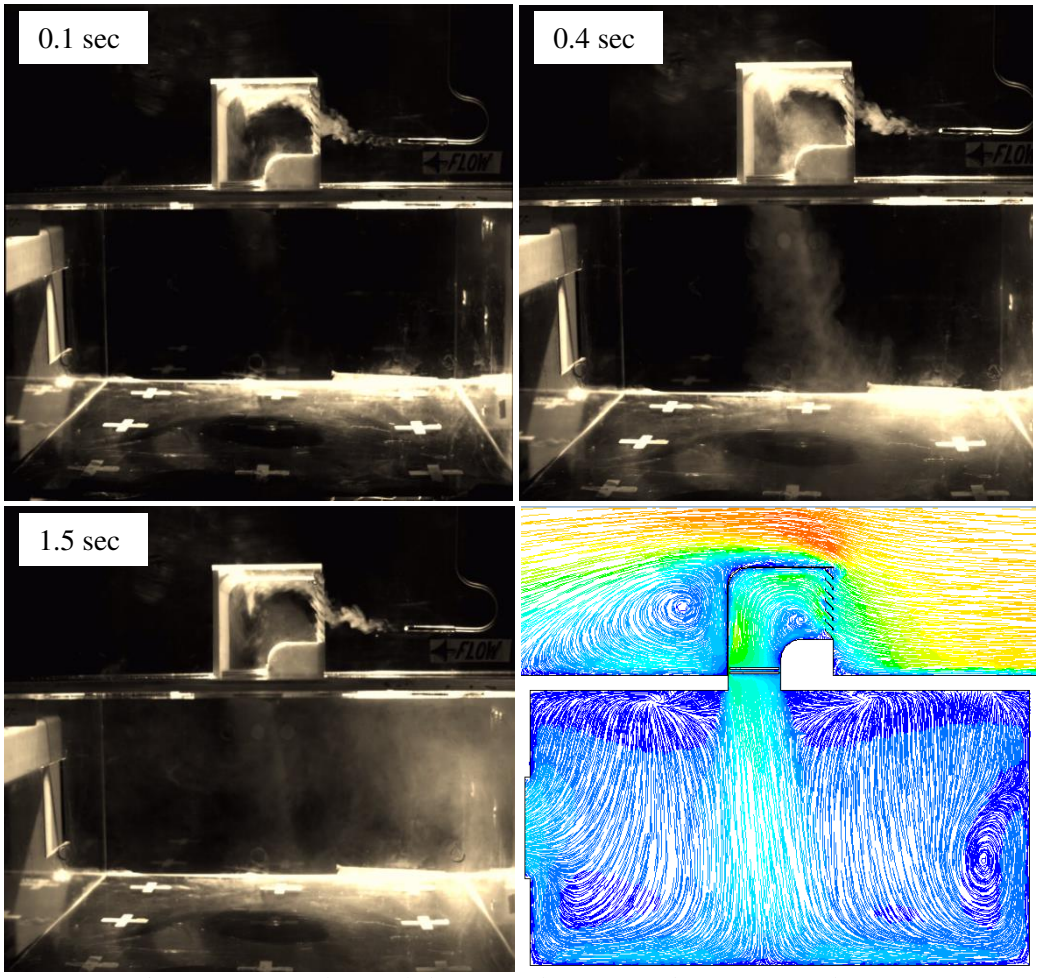

Figure 11: *Wind tunnel flow visualisation and CFD streamlines.*

3.3 Field test results

Figure 12a is an example of the day-time cooling of the wind catcher during a windy and summer day. It shows the external air temperature, heat pipe surface temperature and the temperature downstream of the heat pipes from 11:00 AM to 4:00 PM, September 17, 2014. The cold sink was fed with water every 15 – 20 minutes to maintain the sink temperature at around 293 K. This was initiated when the wind catcher began to deliver airflow inside the room (11:40 AM), although the wind was still mostly out from the West direction at this point. The air temperature decreased by 3 K - 4 K at 12:00 PM when the wind started to flow inside the wind catcher. At 1:00 PM, the wind was blowing more consistently from West-North-West direction (45˚ approach angle) and the reduction was 4 K - 5 K. From 2:00 to 4:00 PM, the wind was parallel to the opening of the wind catcher and the temperature reduction ranged between 2 K - 7 K.

Figure 12b shows the measured outdoor, supply and heat pipe surface temperature from 11:00 AM to 4:00 PM, September 18, 2014. The wind catcher began to deliver airflow into the room at 11:30 AM and the temperature reduction ranged between 3 - 4 K. From 1:00 to 4:00 PM, the wind was blowing mostly from North-West and North-North-East direction and the temperature reduction ranged between 3 K – 11.5 K.

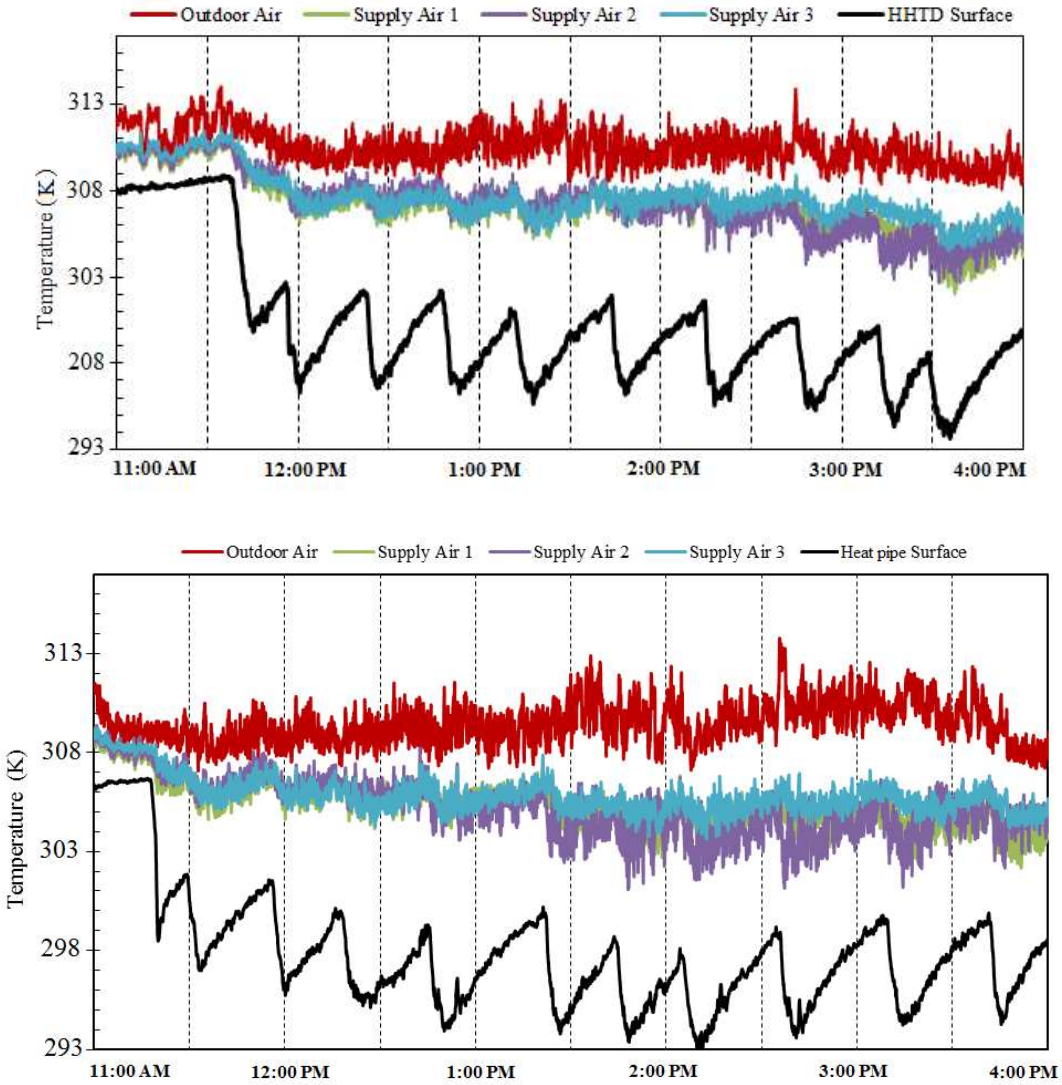

Figure 12: *(a) September 17 testing results from 11:00 to 4:00 (b) September 18 testing results from 11:00 to 4:00*

5 Conclusions

The integration of wind catchers as a low energy alternative to HVAC systems has the potential to improve the thermal comfort of occupants, the indoor air quality and reduce energy consumption and greenhouse gas emissions. In this study, a standard roof-mounted wind catcher was integrated with heat pipes to reduce the temperature of the supply airflow. The work used CFD, wind tunnel analysis and field testing to evaluate the performance of the wind catcher with heat pipes. The CFD model provided detailed analysis of the airflow and temperature distribution inside the wind catcher and also the indoor space. A cooling potential of up to 12 K was identified in this study. Simulation of various outdoor wind speeds showed that the cooling performance of the heat pipes were indirectly proportional to the speed of the outdoor airflow. At 5 m/s outdoor wind speed, the air temperature was only reduced by 5 K - 6 K. While, a higher temperature reduction was observed at lower wind speed, 9.5 K reduction at 2 m/s. The difference between the wind tunnel measurements and CFD results was 10 % on average. Full-scale testing of the wind catcher was carried out to evaluate its performance under real conditions.

Acknowledgement

The support by the University of Leeds and CSEM-UAE are gratefully acknowledged. The statements made herein are solely the responsibility of the authors. The technology presented here is subject to an international patent application (PCT/GB2014/052263).

References

[1] M.M. Rahman, M.G. Rasul , M.M.K. Khan, Energy conservation measures in an institutional building in sub-tropical climate in Australia, Applied Energy 87 (2010) 2994-3004.

[2] Y.H. Yau, S.K. Lee, Feasibility study of an ice slurry-cooling coil for HVAC and R systems in a tropical building, Applied Energy 87 (2010) 2699-2711.

[3] D.O'Connor, J.K. Calautit, B.R. Hughes, A Study of Passive Ventilation Integrated with Heat Recovery, Energy and Buildings (2014) 82 799-811.

[4] B.R. Hughes, J.K. Calautit , S.A. Ghani, The Development of Commercial Wind Towers for Natural Ventilation: a review, Applied Energy 92 (2012) 606-627.

[5] H. Fathy, Natural energy and vernacular architecture: principles and examples with reference to hot arid climates, The University of Chicago Press Chicago and London, 1986.

[6] B.R. Hughes, H.N. Chaudhry, J.K. Calautit, Passive energy recovery from natural ventilation air streams, Applied Energy 113 (2014) 127-140.

[7] J.K. Calautit, B.R. Hughes, S.A. Ghani, A Numerical Investigation into the Feasibility of Integrating Green Building Technologies into Row Houses in the Middle East, Architectural Science Review (2013) 56 279-296.

[8] S. Attia, A. De Herde, Designing the Malqaf for summer cooling in low-rise housing, an experimental study, Conference on Passive and Low Energy Architecture, Quebec City, Canada, 22-24, 2009.

[9] H. Montazeri, R. Azizian, Experimental study on natural ventilation performance of one-sided wind catcher, Building and Environment 43 (2008) 2193–2202.

[10] M. Bahadori, M. Mazidi, A.R, Dehghani, Experimental investigation of new designs of wind towers, Renewable Energy 33 (2008) 2273–2281.

[11] H. Saffari, S . Hosseinnia, Two-phase Euler-Lagrange CFD simulation of evaporative cooling in a Wind Tower, Energy and Buildings 41(2009) 991–1000.

[12] Y. Bouchahm, F. Bourbia, A. Belhamri, Performance analysis and improvement of the use of wind tower in hot dry climate, Renewable Energy 36 (2011) 898-906.

[13] V. Kalantar, Numerical simulation of cooling performance of wind tower (Baud-Geer) in hot and arid region, Renewable Energy 34 (2009) 246–254.

[14] J.K. Calautit, H.N. Chaudhry, B.R. Hughes, S. A. Ghani, Comparison between evaporative cooling and heat pipe assisted thermal loop for a commercial wind tower in hot and dry climatic conditions, Applied Energy 101 (2013) 740-755.

[15] J.K. Calautit, B.R. Hughes, H.N. Chaudhry, S.A. Ghani, CFD analysis of a heat transfer device integrated wind tower system for hot and dry climate, Applied Energy 112 (2013) 576-591.

[16] Modeling of pulsating heat pipe (access date: 2015) available on: http://www.pmmh.espci.fr

[17] P. Sofotasiou, B.R. Hughes, J.K. Calautit, Qatar 2022: Facing the FIFA World Cup climatic and legacy challenges, Sustainable Cities and Society, 14 (2015) 16-30.
[18] J.K. Calautit, D.O'Connor, B.R. Hughes, Determining the optimum spacing and arrangement for commercial wind towers for ventilation performance, Building and Environment 82 (2014) 274-287.
[19] J.K. Calautit, B.R. Hughes, Measurement and prediction of the indoor airflow in a room ventilated with a commercial wind tower, Energy and Buildings, 84 (2014) 367-377.
[20] J.K. Calautit, B.R. Hughes, Wind tunnel and CFD study of the natural ventilation performance of a commercial multi-directional wind tower, Building and Environment, 80 (2014) 71-83.
[21] J.K. Calautit, H.N. Chaudhry, B.R. Hughes, L.F. Sim, A validated design methodology for a closed-loop subsonic wind tunnel, Journal of Wind Engineering and Industrial Aerodynamics 125 (2014) 180-194.
[22] J.K. Calautit, B.R. Hughes, S.A. Ghani, Numerical investigation of the integration of heat transfer devices into wind towers, Chemical Engineering Transactions 34 (2013) 43-48.
[23] J.K. Calautit, D.O'Connor, P. Sofotasiou, B.R. Hughes, CFD Simulation and Optimisation of a Low Energy Ventilation and Cooling System, Computation 3 (2015) 128-149.
[24] J.K. Calautit, B.R. Hughes, S.S. Shahzad, CFD and wind tunnel study of the performance of a uni-directional wind catcher with heat transfer devices, Renewable Energy 83 (2015) 85-99.
[25] J.K. Calautit, Integration and Application of Passive Cooling Within a Wind Tower, Ph.D. Thesis, University of Leeds, Leeds, UK, 2013.